A Stopped-Flow Kinetic Study of the Assembly of Nonviral Gene Delivery Complexes

Chad S. Braun,* Mark T. Fisher,[†] Donald A. Tomalia,[‡] Gary S. Koe,[§] Janet G. Koe,[§] and C. Russell Middaugh*

*Department of Pharmaceutical Chemistry, University of Kansas, Lawrence, Kansas 66047; [†]Department of Biochemistry and Molecular Biology, University of Kansas Medical Center, Kansas City, Kansas 66160; [‡]Dendritic Nanotechnologies, Mt. Pleasant, Michigan 48858; and [§]Valentis Inc., Burlingame, California 94010

ABSTRACT   Stopped-flow circular dichroism and fluorescence spectroscopy are used to characterize the assembly of complexes consisting of plasmid DNA bound to the cationic lipids dimethyldioctadecylammonium bromide and 1, 2-dioleoyl- 3-trimethylammonium-propane and a series of polyamidoamine dendrimers. The kinetics of complexation determined from the stopped-flow circular dichroism measurements suggests complexation occurs within 50 ms. Further analysis, however, was precluded by the presence of mixing (shear) artifacts. Stopped-flow fluorescence employing the high-affinity DNA dyes Hoechst 33258 and YOYO-1 was able to resolve two sequential steps in the assembly of complexes that are assigned to binding/ dehydration and condensation events. The rates of each process were determined over the temperature range of 10–50°C and activation energies were determined from the slope of Arrhenius plots. The behavior of polyamidoamine dendrimers can be separated into two classes based on their differing binding modes: generation 2 and the larger generations (G4, G7, and G9). The larger generations have activation energies for binding that follow the trend G4 > G7 > G9. The activation energies for condensation (compaction) of complexes composed of these same dendrimers have the opposite trend G9 > G7 > G4. It is postulated that a balance between a more energetically favorable condensation and less favorable binding may prove beneficial in enhancing gene delivery.

INTRODUCTION

More than a decade of research into nonviral gene delivery has yielded a number of synthetic cationic lipids and polymers with transfection activity (Boussif et al., 1995; Felgner et al., 1994, 1987; Huang et al., 2002, 1998; Kukowska-Latallo et al., 1996; Murphy et al., 1998; Philip et al., 1993; Zhu et al., 1993). In concert with these efforts, attempts have been made to establish structure/function relationships between polycationic delivery systems and their biological activity (Braun et al., 2003; Choosakoonk-riang et al., 2003a,b, 2001; Dunlap et al., 1997; Golan et al., 1999; Koltover et al., 1998; Lee et al., 2001; Lin et al., 2003; Lobo et al., 2001, 2003, 2002; Radler et al., 1997; Wiethoff et al., 2002, 2003, 2004, 2001). Surprisingly, however, the assembly of polycationic gene delivery complexes has rarely been studied except under equilibrium and near-equilibrium conditions (Lai and van Zanten, 2001, 2002; Tecle et al., 2003). Here we explore temporal aspects of DNA/polymer assembly, employing stopped-flow circular dichroism (CD) and extrinsic fluorescence.

At a minimum, assembly of DNA/polycationic complexes can be viewed to consist of at least two sequential events. First, a spontaneous, electrostatically mediated binding occurs between positively charged amines on polycations with the negatively charged phosphates of the DNA. This produces local and eventually long-range charge neutralization resulting in collapse of the DNA and polycation into a more condensed phase. Cationic lipid/DNA complexes (CLDCs) undergo condensation to a locally ordered phase characterized by stacked arrays of lipid bilayer lamellae between which DNA is sandwiched (Radler et al., 1997). In contrast, polyamine polymers such as polyamidoamine dendrimer/DNA complexes (PDDCs) appears to condense to rod-like or toroidal structures with an underlying square or hexagonal unit cell depending on solution conditions and the chemistry of the individual polycations (Dunlap et al., 1997; Evans et al., 2003; Golan et al., 1999).

The spectroscopic properties of CLDCs and PDDCs at equilibrium have been studied previously. The CD spectra of these complexes are altered significantly from that of unliganded DNA, generally displaying red-shifted peaks of decreased rotational strength characteristics of B-form oligonucleotides (Akao et al., 1996; Braun et al., 2003; Zuidam et al., 1999). The fluorescence of many dyes that bind DNA is altered either through displacement from their binding sites by polycations or by dehydration of the DNA upon formation of complexes (Bhattacharya and Mandal, 1998; Birchall et al., 1999; Eastman et al., 1997; Gershon et al., 1993; Harvie et al., 1998; McKenzie et al., 2000; Wong et al., 2003). By extending these two techniques into the time domain in this study, we attempt to resolve the binding event from the condensation/reorganization process.

To this end, we have examined the formation kinetics of both CLDCs (consisting of dimethyldioctadecylammonium bromide (DDAB) or 1, 2-dioleoyl- 3-trimethylammonium-propane (DOTAP)) and a series of PDDCs (consisting of

generation 2, 4, 7, or 9 polyamidoamine (PAMAM) dendrimer) by stopped-flow circular dichroism and fluorescence spectroscopy. The chemical structures of the cationic lipids and a representative PAMAM dendrimer are shown on the left side of Fig. 1. Cationic lipid/DNA complexes are formed from single unilamellar liposomes of ~100 nm in diameter whereas the various generations of PAMAM dendrimer utilized to form PDDCs vary considerably in size. An illustration of the relative sizes of each cation is represented by a series of circles in Fig. 1. The kinetics of
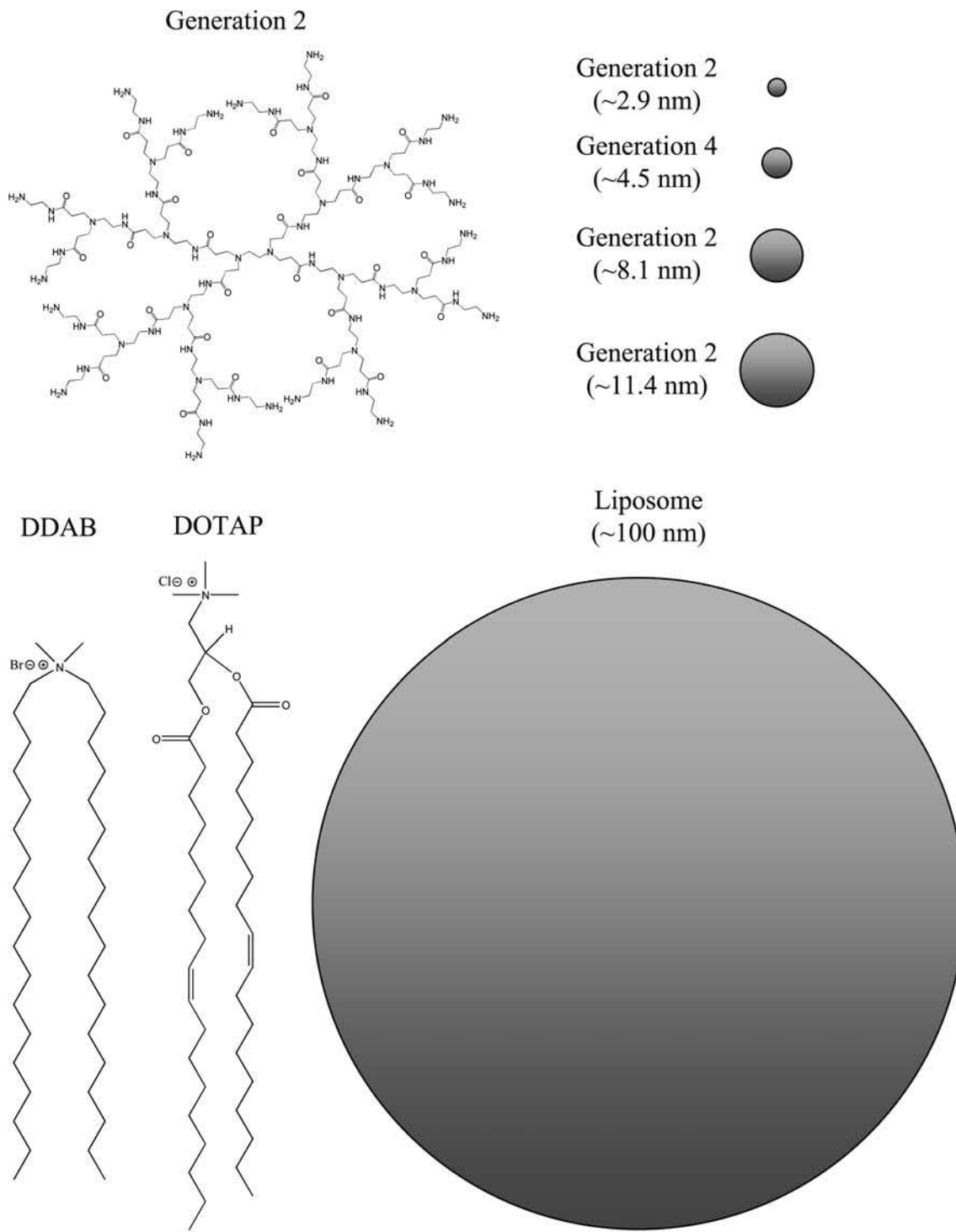

FIGURE 1 Chemical structures of a generation 2 PAMAM dendrimer and the cationic lipids DDAB and DOTAP are shown on the left side of the figure. A series of spheres intended to give an indication of the relative size of each cationic reagent is provided on the right.

formation of complexes from each of these cationic vehicles was studied at five temperatures from 10 to 50°C to derive the activation energy from the temperature dependence of each kinetic phase. The rates derived from exponential fits to the resultant data as well as the associated activation energies (E_a) are discussed in terms of the associated physical events of the complexation process.

MATERIALS AND METHODS

Materials

Plasmid DNA pMB 290 (4.9 kbp, >95% supercoiled) was provided by Valentis (Burlingame, CA). The PAMAM dendrimers of generations 2, 4, 7, and 9 were a gift from Dendritic Nanotechnologies (Mt. Pleasant, MI). The cationic lipids DDAB and DOTAP were obtained from Avanti Polar Lipids (Alabaster, AL) and used without further purification. The fluorescent dyes Hoechst 33258 (HOEC) and YOYO-1 (YOYO) were purchased from Molecular Probes (Eugene, OR) and the MOPS buffer salts from Sigma/Aldrich (St. Louis, MO). Nanopurified water was used for all buffer preparation.

Preparation of complexes

Liposomes were prepared by placing a chloroform solution containing the cationic lipid into a glass vial and evaporating the solvent by use of a stream of nitrogen gas. The lipid film formed was dried for 2.5 h in a desiccator under vacuum. The lipid was then hydrated with 10 mM MOPS buffer, pH 7.4, by vortexing. The resultant liposomes were allowed to equilibrate for 30 min and were then extruded 11 times through a 100-nm pore polycarbonate membrane (Whatman, Clifton, NJ) to form small unilamellar vesicles. Both the hydration and extrusion of lipids were carried out above their relevant phase transition temperatures (i.e., room temperature for DOTAP and 55°C for DDAB). The final size of the liposomes used in all experiments was 105 ± 17 nm as measured by dynamic light scattering.

The dendritic polymers were received at high concentration (>10% w/w) in methyl alcohol. An aliquot of the stock solution was placed into a glass vial and the solvent was removed by evaporation using a stream of dry nitrogen. Removal of the solvent was assured by placing the vial containing the dendrimer under vacuum until a stable weight was achieved. The dendrimer was then hydrated in 10 mM MOPS buffer, pH 7.4, by vortex mixing before analysis. The plasmid was diluted into 10 mM MOPS buffer (pH 7.4) from a stock solution to an appropriate concentration for further analysis. The concentration of DNA solutions was determined using their ultraviolet absorbance at 260 nm (A_{260}) and a molar extinction coefficient of 0.02 (mg^{-1} cm^{-1} ml). Complexes were prepared by stopped-flow mixing from two independent solutions at the time of data collection. The size of the resultant complexes are 245, 105, 172, and 258 nm (±~29 nm) for G2, 4, 7, and 9 dendrimers, respectively, as determined by DLS.

Stopped-flow circular dichroism spectroscopy

Kinetic data were acquired with a stopped-flow CD, PiStar-180 instrument (Applied Photophysics, Surrey, UK). The instrument's optical system was configured with a 75-W xenon lamp, circular light polarizer, and end-mounted photomultiplier. The stopped-flow system was configured with a two-syringe (2.5-ml) kinetic sample handling unit, a 20-μl flow cell (with a 10-mm pathlength), and 2.5-ml stop syringe. Temperature control was achieved through use of a Polyscience digital circulating water bath (Niles, IL). Individual solutions containing pMB 290 (40 μg ml^{-1}) and either DDAB (~58 μg ml^{-1}), DOTAP (~65 μg ml^{-1}) or dendrimer (~20 μg

ml^{-1}) were dispensed into the drive syringes. Formation of 0.75 charge ratio (positive/negative; from here on in the text, all ratios will be of the form +/−) complexes was induced by mixing equal volumes of the two components by stopped-flow addition to the flow cell. Acquisition of CD data was performed at a wavelength of 275 nm over a time frame of up to 30 s with slit widths of 3–10 nm. Before kinetic runs, the flow cell was purged with five 50 μl injections of the solutions to be analyzed. Kinetic data were then acquired as the average of 10 separate 50 μl injections.

Stopped-flow fluorescence spectroscopy

Kinetic fluorescence data were acquired with a PiStar-180 stopped-flow fluorimeter (Applied Photophysics). The optical system employed a 75-W xenon lamp, optical cut-off filters appropriate for the dye used, and an emission photomultiplier mounted 90° from the excitation light path. The kinetic sampling unit was identical to that described above. Temperature control was achieved through use of a Polyscience digital circulating water bath. The plasmid DNA (~20 μg ml^{-1}) was associated with the DNA binding dye Hoechst 33258 (excitation 352 nm, emission 462 nm) at a ratio of 1 dye molecule per 150 basepairs (bp) or with YOYO-1 (excitation 491 nm, emission 509 nm) at a ratio of 1 dye molecule per 50 basepairs. Individual solutions containing the cationic vehicles DDAB (~233 μg ml^{-1}), DOTAP (~129 μg ml^{-1}), or dendrimers (~40 μg ml^{-1}) were transferred with fluorescently labeled DNA to the appropriate instrument drive syringe. Although polyamidoamine dendrimers have been reported to spontaneously fluoresce the fluorescence is highly pH dependent and can be essentially neglected above a pH of 6 (Wang and Imae, 2004). Complexes of charge ratio 3 (+/−) were formed for DOTAP CLDCs and all PDDCs whereas DDAB CLDCs were formed at a charge ratio of 6 (+/−) to avoid the colloidal instability present with the latter liposomes (Braun et al., 2003).

Kinetic data were acquired as the average of five 50 μl injections. Instrument parameters for Hoechst-33258-labeled DNA consisted of excitation at 352 nm, a slit width of 0.5 nm, and a long pass 395-nm optical filter (Oriel, Stratford, CT). The instrument parameters for YOYO-1-labeled DNA employed excitation at 470 nm, a slit width of 0.3 nm, and a long pass 495-nm optical filter. Data were collected at a rate of 800 points over a 2 s interval.

Data analysis was performed using Origin 7 software (Northampton, IL). Kinetic data were fit by a nonlinear least-squares method to a biexponential relationship (Eq. 1) with the exception of experiments with HOEC G2/DNA complexes at high temperatures (40 and 50°C) that were best fit to a mono-exponential form:

$$y = A_1 e^{-k_1 t} + A_2 e^{-k_2 t} + y_0. \tag{1}$$

Calculated rate constants were plotted according to a linear form of the Arrhenius equation (Eq. 2):

$$\ln y = \frac{-E_a}{RT} + \ln A. \tag{2}$$

A linear least-squares fit was performed and the activation energy for each kinetic event was estimated from the slope.

RESULTS

Stopped-flow circular dichroism

Circular dichroism has been shown to sensitively monitor the formation of many gene delivery complexes through changes in the rotational strength of several spectral peaks of the DNA component (Akao et al., 1996; Braun et al., 2003; Choosakoonkriang et al., 2003a). The most prominent change in the CD spectrum as the DNA is complexed is

a reduction (≥30%) in the intensity of the characteristic B-form ellipticity peak at 275 nm. The maximal spectral change for the cationic reagents employed here occurs when the cationic charge is slightly less than theoretical charge neutrality (0.75) (Braun et al., 2003). In fact, our stopped-flow investigations of DNA complexing to both cationic lipids (DDAB and DOTAP) and PAMAM dendrimers (generations 2, 4, 7, and 9) provided little useful kinetic data. Kinetic plots of the intensity of the 275 nm B-form peak of DNA show only a sharp downward spike centered at ∼40–50 ms (Fig. 2). This abrupt spectral change, however, occurs in controls consisting of DNA mixed with buffer. Because this time-dependent spectral feature appeared in the absence of any cationic ligand, we believe it arises from either a shear-induced alteration of base stacking within the DNA upon injection into the flow cell (Crook et al., 1996; Levy et al., 2000) or residual Schlieren optical effects from the mixing process itself. We further conclude that the reduction in rotational strength expected from formation of nonviral complexes (and seen in complexes removed from the mixing chamber) occurs within the ∼40–50 ms time frame in which shear-induced effects predominate. A comparison of agarose gel electrophoretic banding patterns before and after stopped-flow analysis shows no discernible difference suggesting that any alteration in the CD is a temporary effect and does not reflect fragmentation or loss of supercoiling in the plasmid (data not shown).

Hoechst 33258 as a probe of DNA/cation association kinetics

To examine the kinetics of complexation between DNA and the cationic vehicles, Hoechst 33258, a minor groove binding dye, was used as a probe. It has been previously shown that H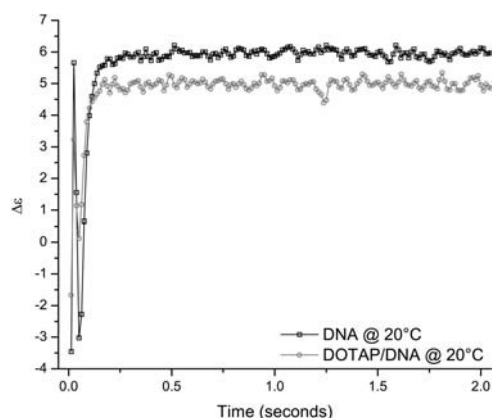OEC remains bound in the DNA minor groove when DNA is complexed with cationic lipids (Wiethoff et al., 2003). This property combined with the sensitivity of its fluorescence to environmental polarity makes HOEC an effective probe of the kinetics of binding of cationic lipids to DNA. Some degree of dye displacement is expected with PAMAM dendrimers based on studies that find displacement of ∼50% of the dye by another polyamine, polyethyleneimine (PEI) (Wiethoff et al., 2003). We found, however, that the fraction of HOEC that remains bound is sufficient to assess PAMAM dendrimer association as well. Representative kinetic traces of the change in relative fluorescence intensity during the first 2 s of the binding of DNA to dendrimers and cationic lipids are shown in Fig. 3, A–D. Kinetic traces of DNA diluted with 10 mM MOPS buffer (pH 7.4) and the formation of G2 dendrimer/DNA complexes are shown in Fig. 3, A and B, respectively. The similarity of the DNA alone and G2 dendrimer/DNA complex traces suggests that G2 is unable to displace HOEC at temperatures ≤30°C. At the higher temperatures examined (40 and 50°C), the slope of the initial phase is negative, indicating a loss of relative fluorescence intensity consistent with displacement of the Hoechst 33258 dye. Shear-induced perturbation is again apparent under 1:1 DNA dilution conditions (Fig. 3 A) as reduced fluorescence intensity. Nevertheless, good biexponential fits could be achieved by neglecting the data at ≤40 ms. The kinetics of G4 dendrimer/DNA complex formation (Fig. 3 C) is typical of PDDCs formed from the higher generations of PAMAM dendrimers. The sharp reduction in fluorescence intensity observed during G4/DNA complex formation presumably reflects a displacement of the HOEC from the minor groove of the DNA. In contrast, an initial increase in fluorescence intensity concomitant with formation of DOTAP/DNA CLDCs suggests that HOEC remains in the minor groove and experiences a more apolar environment during association with the liposome. A second kinetic phase, however, manifests a reduction in fluorescence intensity perhaps related to a rearrangement of the complex inducing dye displacement. The G4/DNA and DOTAP/DNA complexes were chosen for further investigation due to their higher transfection efficiency (Bielinska et al., 1999; Braun et al., 2005; Kukowska-Latallo et al., 1996; Wiethoff et al., 2004).

The rates and associated errors of biexponential fits derived from the assembly kinetics of various PDDCs and CLDCs are summarized in Table 1. The two rates (k_1 and k_2) listed in Table 1 correspond to the two phases described earlier. The initial rate (k_1) for G2 PDDC formation appears to resemble the shear effect observed in DNA control kinetic experiments at temperatures between 10 and 30°C and was therefore neglected in further analysis. At temperatures ≥40°C, an initial loss in fluorescence intensity and a rate similar to that seen with higher generation PDDCs is apparent. This may indicate displacement of HOEC under these conditions. This initial rate was fit to a single exponential and reported as such. In fitting the CLDCs kinetic data, the initial
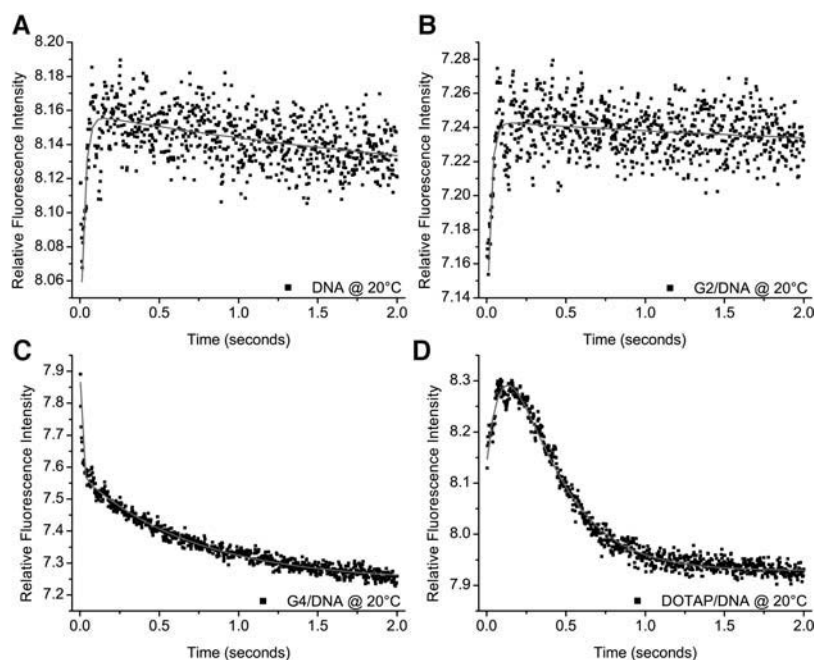

FIGURE 2 Representative stopped-flow CD kinetic plots monitored at a wavelength of 275 nm for DNA alone (□) and DOTAP/DNA complexes (○). The kinetic plots were acquired at 20°C for 2 s as the average of 10 individual injections.

FIGURE 3 Representative stopped-flow fluorescence data for Hoechst 33258 (1:150 dye/bp) labeled DNA (*A*), G2 dendrimer/DNA complexes (*B*), G4 dendrimer/DNA complexes (*C*), and DOTAP/DNA complexes (*D*). Each kinetic trace was acquired at 20°C for 2 s as the average of five individual injections. The trend line is a biexponential fit of the data.

rate (k_1) corresponding to apparent association appears to occur too quickly to be measured at elevated temperature (40–50°C for both DDAB and DOTAP CLDCs) and therefore is not presented in the table.

The rates derived from the biexponential fits of PDDCs are plotted as a series of Arrhenius plots in Fig. 4 with the resulting activation energy indicated in bold type in the plots. The dendrimer/DNA complexes display an activation energy for k_1 following the trend of G9 > G7 > G4. The activation energies derived from k_2 are significantly greater than those associated with k_1 but show the similar trend of G9 ~ G7 > G4. Although the activation energy for release of HOEC from the kinetics of G2 PDDC formation is based on only two points, we calculated an approximate E_a value of 13 kcal mol^{-1} (data not shown). This G2/DNA activation energy has only limited utility, however, because we cannot unambiguously assign it to either the fastest (k_1) or slower (k_2) rate process.

The rates derived for formation of CLDCs are similarly plotted as Arrhenius plots in Fig. 5. The activation energies associated with k_1 indicate a much higher (14 kcal mol^{-1}) activation energy for DOTAP CLDCs than DDAB (3 kcal mol^{-1}). In contrast, the activation energies for the second rate process are higher for DDAB (27 kcal mol^{-1}) than DOTAP (8 kcal mol^{-1}) complexes.

YOYO-1 as a probe of DNA/cation formation kinetics

YOYO-1 is a dimeric intercalating dye that remains associated with DNA upon complexation with cationic lipids and polyamines (Krishnamoorthy et al., 2002;

Wiethoff et al., 2003; Wong et al., 2001; Zaric et al., 2004). Intercalating dyes (e.g., ethidium bromide) have seen extensive use as probes to measure the conformational perturbation (condensation) of DNA when bound to a variety of nonviral gene delivery agents (Bhattacharya and Mandal, 1998; Choosakoonkriang et al., 2003a; Eastman et al., 1997; Gershon et al., 1993). Representative kinetic traces of changes in the fluorescence of YOYO-1 DNA bound dye upon formation of PDDCs (G4/DNA) and CLDCs (DOTAP/DNA) are illustrated in Fig. 6. A kinetic trace of YOYO-labeled DNA undergoing dilution shows a rapid loss of fluorescence intensity related to shear-induced alteration of DNA structure (Fig. 6 *A*). The rapid initial increase in fluorescence intensity followed by an eventual decrease during G4/DNA PDDC formation (Fig. 6 *B*) suggests the early phase may be related to DNA-dendrimer binding. It has been suggested previously that polyamine binding results in dehydration of the DNA, which could explain the increase in fluorescence intensity (Choosakoonkriang et al., 2003a; Wiethoff et al., 2003). The later kinetic phase, characterized by a reduction in fluorescence intensity, probably reflects rearrangement to a more compact structure and quenching of dye fluorescence or exclusion of the dye from its intercalated binding site. The kinetics of formation G2/DNA PDDCs show the initial (k_1) phase but no decrease in fluorescence intensity over the 2 s time frame examined. This again suggests that the G2 dendrimer is incapable of displacing YOYO-1 (data not shown). The representative CLDC kinetic trace (Fig. 6 *C*) shows a brief period of reduced fluorescence intensity (<~40 ms), again presumably related to shear effects, followed by an increase in fluorescence intensity that was fit to a biexponential rate equation. The kinetic phase

TABLE 1 Kinetics of complexation as monitored by Hoechst 33258 dye vehicle

	Temperature	k_1 (s^{-1})	±SD	k_2 (s^{-1})	±SD
G2	10°C	n/a*	n/a	n/a	n/a
	20°C	n/a	n/a	n/a	n/a
	30°C	n/a	n/a	n/a	n/a
	40°C	67.2	10.3	n/a	n/a
	50°C	129.7	13.6	n/a	n/a
G4	10°C	70.3	111.0	0.6	0.05
	20°C	99.1	6.9	1.4	0.03
	30°C	186.6	12.9	3.7	0.05
	40°C	211.4	22.8	10.3	0.2
	50°C	268.1	45.3	23.2	1.0
G7	10°C	30.3	1.1	0.4	0.02
	20°C	37.5	1.0	1.2	0.02
	30°C	51.3	1.5	2.6	0.04
	40°C	107.2	4.4	8.5	0.2
	50°C	177.3	25.1	31.0	2.2
G9	10°C	12.2	0.3	0.7	0.04
	20°C	19.0	0.3	1.3	0.04
	30°C	29.3	0.5	2.5	0.05
	40°C	68.5	2.5	11.5	0.4
	50°C	139.5	22.8	36.6	3.5
DDAB	10°C	11.6	0.5	0.2	0.1
	20°C	14.7	0.8	0.2	0.04
	30°C	16.4	1.0	1.5	0.03
	40°C	n/a	n/a	11.5	0.3
	50°C	n/a	n/a	41.3	1.5
DOTAP	10°C	3.9	0.5	2.6	0.3
	20°C	8.2	0.4	3.5	0.1
	30°C	19.8	1.1	4.6	0.1
	40°C	n/a	n/a	10.5	0.4
	50°C	n/a	n/a	12.4	0.2

*The not applicable (n/a) designation represents data that were neglected because they could not be unambiguously assigned to either kinetic phase.

characterized by an increasing fluorescence signal should reflect lipid-DNA binding.

The rates and associated experimental errors derived from biexponential fits are presented in Table 2. The rates for PDDC formation are plotted as a series of Arrhenius plots with the derived activation energy shown in the individual plots (Fig. 7). The magnitude of the activation energy derived from the initial kinetic rates follows the trend of G4 > G7 > G9 > G2. The activation energy derived from the second kinetic rate constant (k_2) shows a trend similar to that observed for HOEC monitored assembly (i.e., G9 > G7 > G4 > G2). Arrhenius plots associated with CLDCs assembly kinetics are described in Fig. 8. The activation energies calculated from the initial rate (k_1) are nearly the same for DDAB and DOTAP CLDCs. The second kinetic phase (k_2) does not appear to be well fit by a single line but is better approximated by two line segments, one at or above 40°C and a second below.

DISCUSSION

The spectral properties of both DNA and fluorescent dyes bound to DNA are significantly altered upon formation of complexes of DNA with cationic liposomes and dendritic polymers (Akao et al., 1996; Braun et al., 2003, 2005; Wiethoff et al., 2003). On this basis, the kinetics of formation of cationic lipid/DNA complexes composed of DDAB or DOTAP and PAMAM dendrimer/DNA complexes (G2, 4, 7, and 9) were explored by monitoring spectral changes in a stopped-flow mode. Circular dichroism was used to directly evaluate conformational changes within DNA itself whereas changes in extrinsic dye fluorescence were employed to investigate both binding processes and condensation of the DNA within complexes.

Stopped-flow CD spectroscopy

Stopped-flow CD kinetic traces of the assembly of both CLDCs and PDDCs were dominated by a sharp decrease in the ellipticity at the wavelength of the major CD maximum (275 nm), with the change maximal at ~40–50 ms. Nearly identical kinetic traces were observed when DNA was simply diluted. As discussed above, this sharp reduction in rotational strength is probably related to a shear-induced perturbation of the base-stacking interactions of the plasmid. This explanation is consistent with observations from the plasmid processing literature in which shear-induced tertiary structural changes have been reported for plasmid DNA (Anchordoquy et al., 1998; Lengsfeld and Anchordoquy, 2002; Levy et al., 1999, 2000). Agarose gel electrophoresis of the plasmid before and after being subjected to stopped-flow shear confirmed the extent of supercoiling remained constant suggesting the perturbation is transient. Unfortunately, the predicted stopped-flow CD changes associated with the formation of both CLDCs and PDDCs seen in equilibrium experiments occurred within the ~100 ms time period over which this shear-induced effect predominates. Therefore, we can only conclude that the early binding events that produce the conformation changes reflected in the loss of rotational strength occur within 100 ms. A similar sub-100-ms time for binding of a fluorescent peptide has been found previously in a stopped-flow fluorescence study of cationic peptide/DNA assembly (Tecle et al., 2003).

Stopped-flow fluorescence spectroscopy

High-affinity DNA binding fluorescent dyes have made important contributions to the brief history of the study of nonviral gene delivery (Bhattacharya and Mandal, 1998; Birchall et al., 1999; Chen et al., 2000; Gershon et al., 1993; Harvie et al., 1998; Richter-Egger et al., 2001). We combined the use of two such probes with different binding modes to investigate the formation kinetics of both CLDCs and PDDCs. For this purpose, Hoechst 33258, a minor groove binding dye, and YOYO-1, a bisintercalating dye were employed. The dye/basepair (dye/bp) ratio used to label the DNA was based on preliminary studies to assure
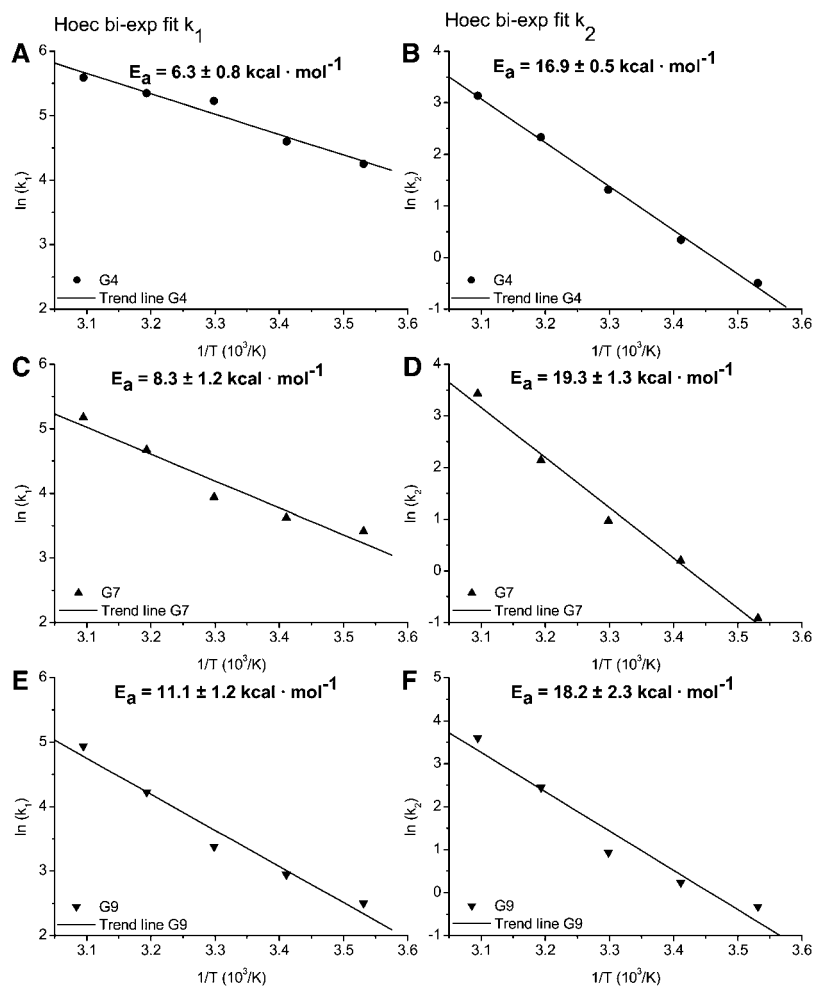
FIGURE 4 Arrhenius plots of the two rate processes derived from biexponential fits of the stopped-flow fluorescence of PDDCs labeled with Hoechst 33258. The individual Arrhenius plots are G4/DNA complexes (*A* and *B*), G7/DNA complexes (*C* and *D*), and G9/DNA complexes (*E* and *F*). The slope generated from a linear fit of the data is given as the activation energy (E_a) in bold type in each panel.

a homogenous binding mode for each dye. Hoechst 33258 was associated with DNA at a 1:150 dye/bp ratio to promote preferential binding to AT-rich regions and minimize the potential for dye displacement (Wiethoff et al., 2003). YOYO-1 was associated with DNA at a 1:50 dye/bp ratio at which the binding mode is exclusively bisintercalation (Larsson et al., 1994; Rye et al., 1992) and no energy transfer or self-quenching occurs (Cosa et al., 2001).

In contrast to the CD kinetic studies, the stopped-flow induced shear is only modestly reflected in the extrinsic fluorescence changes. When DNA labeled with either dye was diluted by stopped flow, the fluorescence undergoes a rapid change in intensity followed by a slower recovery of the fluorescence intensity. The magnitude of this shear-induced fluorescence change is small but significant with respect to the changes occurring during formation of CLDCs and PDDCs. The presence of the cationic reagents affects the rate of DNA recovery to its equilibrium state. Therefore, this shear-induced effect cannot be deconvoluted from the complexation kinetics and must be considered in the interpretation of the data described below.

Hoechst 33258 as a probe of nonviral gene delivery complex formation

The kinetics of formation of PDDCs and CLDCs differ in that the initial kinetic phase (k_1) for PDDCs undergoes a rapid biexponential loss of fluorescence intensity whereas CLDCs induce increasing intensity followed by a modest decrease in fluorescence. This result agrees with the observation that HOEC remains substantially bound within CLDCs but is displaced by polyamines such as PEI (Wiethoff et al., 2003). In the case of PDDC formation, both the k_1 and k_2 phases are associated with a rapid loss of fluorescence intensity commonly assigned to displacement of HOEC from its DNA binding site (Wiethoff et al., 2003). This occurs due to the ~30-fold difference in quantum yield between HOEC bound to DNA and free in solution (Cosa et al., 2001). In a related manner, the intercalating dye (ethidium bromide) is displaced from DNA during formation of PDDCs (Braun et al., 2005). The modest reduction in fluorescence intensity observed in the second phase of CLDC formation seems to be due to HOEC displacement.
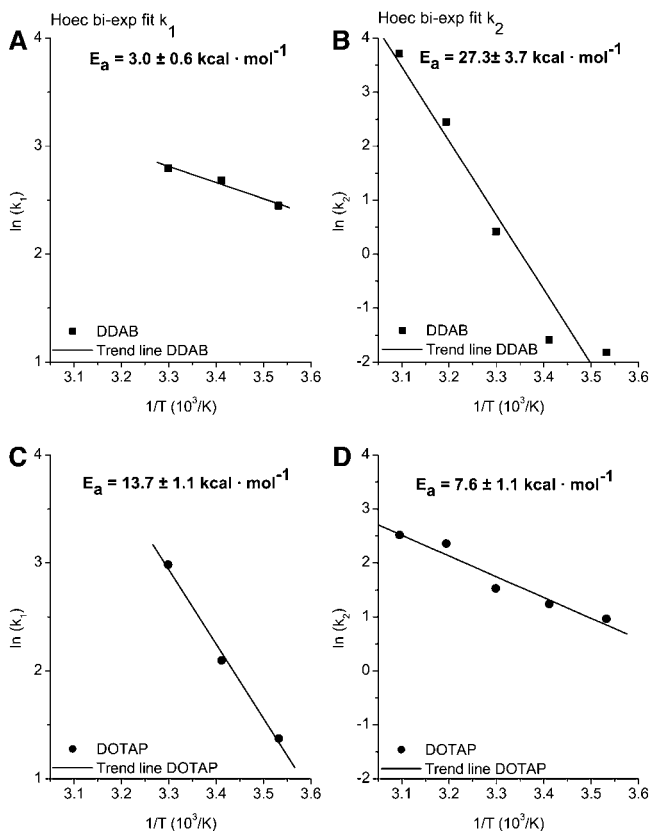
FIGURE 5 Arrhenius plots of the two rates derived from biexponential fits of the stopped-flow fluorescence of CLDCs labeled with Hoechst 33258. The individual Arrhenius plots are DDAB/DNA complexes (A and B) and DOTAP/DNA complexes (C and D). The slope generated from a linear fit of the data is given as the activation energy (E_a) in bold type in each panel.

The smaller apparent dye displacement seen with CLDCs compared to PDDCs is consistent with the extent of HOEC displacement observed in equilibrium studies (Wiethoff et al., 2003). The initial phase of CLDC formation is characterized by a small increase in fluorescence intensity that presumably reflects the initial binding of the lipids to DNA. This results in a reduction in the polarity of the environment of the bound dye and a consequent increase in fluorescence intensity. This increase is modest and therefore the contribution of the recovery of the DNA equilibrium state may influence this rate. With regard to the binding event, it has been argued on the basis of a number of Fourier transform infrared (FTIR) studies that DNA is dehydrated as a consequence of the formation of electrostatically assembled nonviral gene delivery systems (Choosakoonkriang et al., 2003a, 2001; Wiethoff et al., 2003). Furthermore, it has been previously shown that a significant blue shift in the HOEC fluorescence peak in CLDCs is accompanied by a >25% increase in intensity suggesting these spectral changes are directly related to dehydration of the DNA site where HOEC is bound (Wiethoff et al., 2003). The CD studies reported here and in a previous report utilizing

a fluorescent peptide show that the initial binding event occurs in <100 ms. This implies that the event related to dye dehydration consists of at least two steps involving both a binding and release of water through a reorganization step (Tecle et al., 2003).

YOYO-1 as a probe of nonviral gene delivery complex formation

The response of YOYO-1 to the formation of both PDDCs and CLDCs includes an initial phase marked by an increase in fluorescence intensity. This early phase is presumably due to the binding/dehydration event. The appearance of this early binding phase at the low dye/bp ratio of 1:50 suggests the dye remained predominately bound (Cosa et al., 2001; Larsson et al., 1994). The fact that PDDCs show this early phase in contrast to the results obtained with HOEC suggests dehydration occurs with polyamine polymers as well (Choosakoonkriang et al., 2003a; Wiethoff et al., 2003). The assembly of higher generation (G4, 7, and 9) DNA/dendrimer complexes includes an additional kinetic phase (k_2) characterized by a decrease in fluorescence intensity. Although it is tempting to assign this later phase to dye displacement, it is also possible fluorescence quenching upon condensation of the complexes may account for the fluorescence loss. Although both mechanisms appear feasible, we favor the quenching hypothesis because the shortest measured fluorescence lifetime remained much longer (by a factor of 5) when DNA containing YOYO-1 was condensed with PEI than the lifetime of the dye free in solution (Krishnamoorthy et al., 2002; Wong et al., 2001). The series of dendrimers used in these studies have also been reported to condense DNA into small particles with a toroidal structure (Bielinska et al., 1997; Braun et al., 2005). It should be noted that quenching does not require overall collapse into small dense particles but can also be accomplished by localized condensation near dye binding sites. Therefore, we assume the second kinetic phase of PDDC formation provides the best measure of the condensation event. Neither G2/DNA PDDCs nor CLDCs show a reduction in fluorescence intensity within the 2 s period examined. This suggests that the degree of condensation is less for these polycations than for higher generation PAMAM dendrimers. The finding that generation size correlates with an increased ability to displace fluorescent dyes has been reported previously with the intercalating dye ethidium bromide (Braun et al., 2005; Chen et al., 2000).

Activation energies

Based on assignment of each kinetic phase to particular molecular events, we can apply this interpretation to the related activation energies. Using HOEC as a probe, only the first kinetic phase (k_1) of CLDCs appears representative of the binding/dehydration event. The results with YOYO were
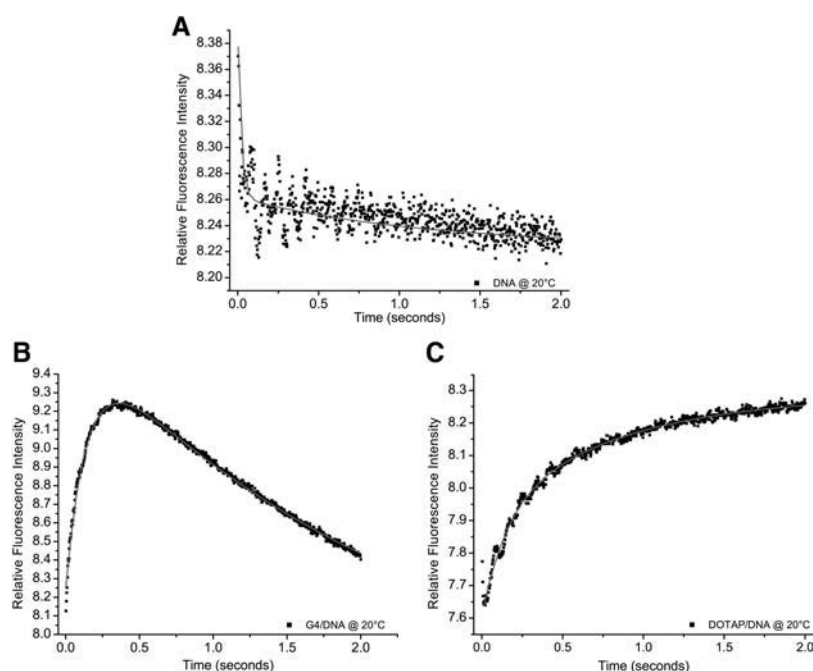
FIGURE 6 Representative stopped-flow fluorescence data for YOYO-1 (1:50 dye/bp) labeled DNA (*A*), G4/DNA complexes (*B*), and DOTAP/DNA complexes (*C*). Each kinetic trace was acquired at 20°C for 2 s as the average of five individual injections. All data were fit to a biexponential function.

used to calculate rates (k_1) for the binding/dehydration event of both cationic lipids and dendrimers. The higher generation PDDCs (G4, 7, and 9) have activation energies that follow the trend of G4 > G7 > G9 and values ranging from 15.7 to

TABLE 2 Kinetics of complexation as monitored by YOYO-1 dye

Vehicle	Temperature	k_1 (s^{-1})	±SD	k_2 (s^{-1})	±SD
G2	10°C	3.2	0.4	0.9	0.5
	20°C	5.8	0.2	1.3	0.06
	30°C	8.3	0.5	1.6	0.08
	40°C	10.5	0.4	1.3	0.07
	50°C	14.2	0.5	1.2	0.05
G4	10°C	2.1	0.2	0.3	0.2
	20°C	7.0	0.1	0.4	0.02
	30°C	15.2	0.3	1.2	0.01
	40°C	33.9	0.9	2.8	0.03
	50°C	69.8	5.1	3.4	0.05
G7	10°C	4.4	0.1	0.3	0.1
	20°C	7.7	0.2	0.6	0.04
	30°C	19.8	0.3	0.9	0.01
	40°C	45.0	0.8	2.6	0.01
	50°C	85.0	4.0	5.5	0.06
G9	10°C	8.2	0.2	0.2	0.9
	20°C	12.0	0.3	0.6	0.1
	30°C	21.7	0.7	0.8	0.02
	40°C	41.3	0.7	2.3	0.02
	50°C	95.5	3.9	5.5	0.1
DDAB	10°C	4.0	0.4	0.9	0.1
	20°C	6.7	0.4	1.2	0.1
	30°C	11.4	0.6	1.9	0.1
	40°C	22.4	0.7	1.4	0.2
	50°C	48.8	15.7	1.6	0.1
DOTAP	10°C	1.5	0.3	4.3	22.5
	20°C	2.7	0.3	5.6	2.7
	30°C	4.2	0.3	11.0	9.8
	40°C	10.7	0.5	0.8	0.2
	50°C	12.4	0.7	1.1	0.1

11.1 kcal mol^{-1}. The remaining PAMAM dendrimer (G2) has a binding activation energy (6.5 kcal mol^{-1}) nearly half that of the higher generations. In addition, the slope of the latter phase (k_2) changes from positive in the case of the G2 dendrimer to negative with the higher generation complexes. These differences suggest a different binding mode for G2, a conclusion drawn in previous equilibrium fluorescence dye studies (Chen et al., 2000). The CLDCs show similar activation energies (DDAB 11.2 kcal mol^{-1} and DOTAP 10.3 kcal mol^{-1}) to those of the higher generation PDDCs. The activation energies of binding for CLDCs derived from HOEC (DDAB 3.0 kcal mol^{-1} and DOTAP 13.7 kcal mol^{-1}) do not correspond well with those derived from the YOYO studies. The low HOEC activation energy for DDAB binding is inconsistent with the values derived for DOTAP CLDCs or those from YOYO studies. This discrepancy could arise from differing degrees of DNA dehydration upon binding between the two lipids. Both fluorescence and FTIR studies at equilibrium, however, suggest the degree of dehydration of DDAB and DOTAP is similar (Choosa-koonkriang et al., 2001; Wiethoff et al., 2003). It thus seems more likely that differences in the intrinsic nature of the oligonucleotide/polycation interaction between the lipids account for the activation energy discrepancy. DDAB and DOTAP differ in both the size of their headgroups and the degree of saturation of their hydrophobic tails. It has been observed in thermal stability and FTIR studies that the larger headgroup of DOTAP has a greater destabilizing effect on DNA structure and a greater degree of interaction with the nucleotide bases (Lobo et al., 2002). Although DDAB is in a gel phase and DOTAP a more fluid liquid crystalline bilayer state in the temperature range (10–30°C) from which the activation energies were determined, it seems more likely
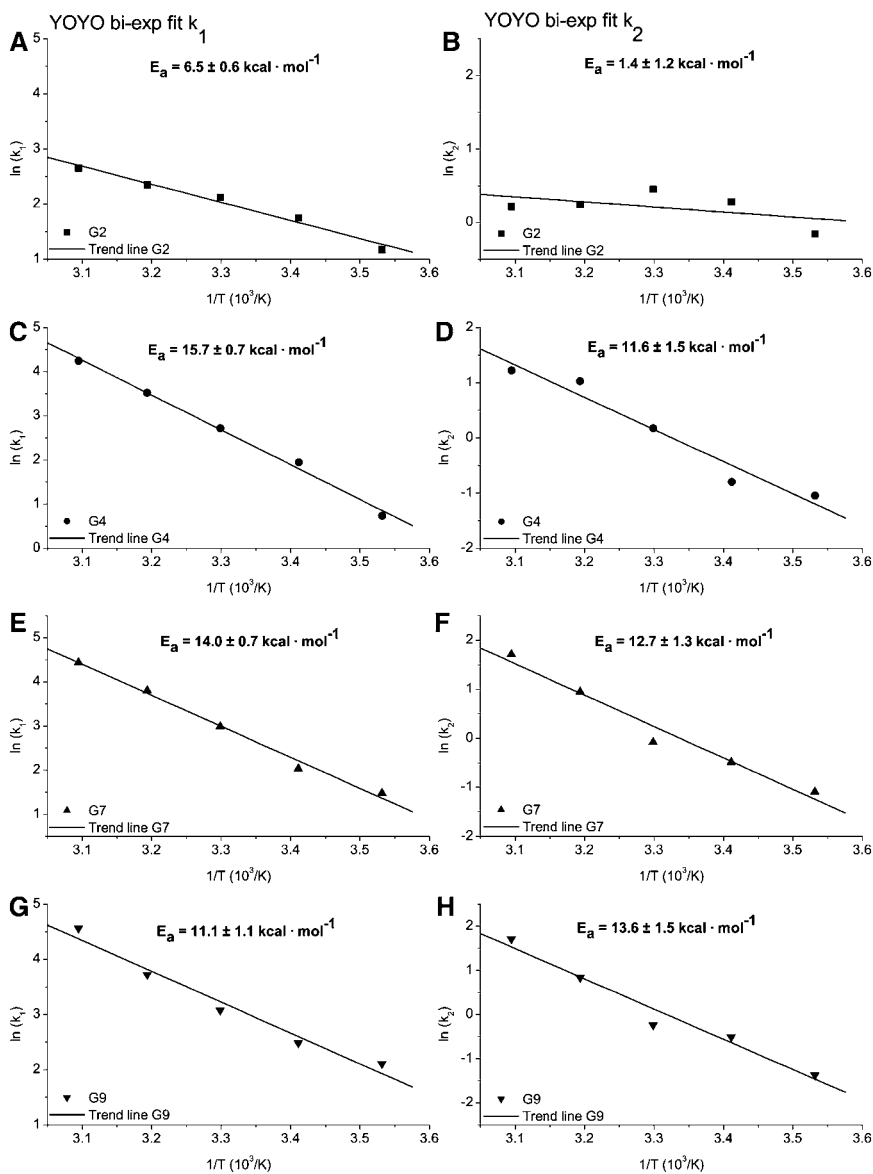
FIGURE 7 Arrhenius plots of the rate constants derived from biexponential fits of the stopped-flow fluorescence of PDDCs labeled with YOYO-1. Individual Arrhenius plots are shown for G2/DNA complexes (*A* and *B*), G4/DNA complexes (*C* and *D*), G7/DNA complexes (*E* and *F*), and G9/DNA complexes (*H* and *I*). The slope generated from a linear fit of the data is given as the activation energy (E_a) in bold type in each panel.

that headgroup chemistry dominates the binding event given the surface location of these moieties (Lobo et al., 2002). That a similar trend is not apparent in activation energies derived from YOYO fluorescence suggests DDAB may have a preferential interaction with HOEC or its minor groove binding site.

The secondary condensation event was best observed during PDDC formation. Activation energies of all the polycations were determined from the HOEC fluorescence studies. The activation energies for PDDCs follow the trend G9 > G7 > G4, which suggests the activation energy barrier is higher for larger PAMAM dendrimers. This same trend is observed for the activation energies determined by YOYO monitored condensation. The only significant difference between the HOEC and YOYO studies is that the average activation energy is ~4 kcal mol^{-1} more for YOYO. These

higher activation energies suggest that a greater degree of condensation is necessary to quench YOYO fluorescence than to displace the HOEC dye. The displacement of HOEC by G2 PAMAM dendrimers at 40 and 50°C suggests that HOEC binding is weaker at elevated temperature.

In the case of CLDCs, no kinetic event related to YOYO quenching (condensation) was observed. Although as argued earlier it seems likely only a small fraction of HOEC is displaced by CLDCs, the trend in activation energies of DDAB ≫ DOTAP suggests a difference in the structure of the CLDCs formed. Hoechst 33258 and FTIR studies do show differences between the two lipids, which may be related to differential condensation. Equilibrium Hoechst 33258 studies confirm DOTAP dehydrates the DNA to a greater extent than DDAB. At high dye/DNA (1:25) loading, however, DDAB complexes of high charge
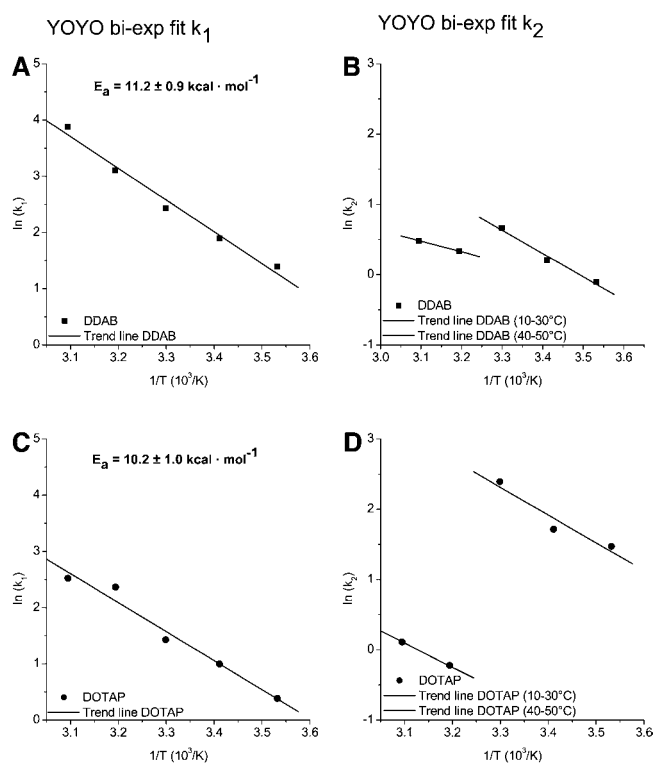
FIGURE 8 Arrhenius plots of the two rate constants derived from biexponential fits of the stopped-flow fluorescence of CLDCs labeled with YOYO-1. Individual Arrhenius plots are shown for DDAB/DNA complexes (*A* and *B*) and DOTAP/DNA complexes (*C* and *D*). The slope generated from a linear fit of the data is given as the activation energy (E_a) in bold type in each panel. The second rate constant (k_2) of CLDC formation could not be fit to a straight line and consequently the activation energy is not given.

ratio (>2) have a higher fluorescence intensity (Wiethoff et al., 2003). This suggests DOTAP complexes lose intensity through dye displacement during condensation whereas the dye within DDAB complexes remains bound. Additionally, the frequency of both the asymmetric phosphate stretching band (1223 cm^{-1}) and the base carbonyl stretching vibration (1715 cm^{-1}) increases more when complexed to DOTAP than DDAB (Choosakoonkriang et al., 2001). Together, these observations suggest that DOTAP may condense DNA to a greater degree than DDAB and that is reflected in a stronger interaction. The difference in headgroup between the two lipids, however, may also contribute to these effects. Because the condensation event involves structural rearrangement of the complexes, the difference in activation energies between DDAB (27 kcal mol^{-1}) and DOTAP (8 kcal mol^{-1}) may arise from the difference in their bilayer properties. A number of studies show that DDAB CLDCs are significantly larger than DOTAP complexes suggesting a reduced degree of compaction in the former (Braun et al., 2003; Choosakoonkriang et al., 2001; Lobo et al., 2001).

CONCLUSIONS

Previous attempts to establish a structure/activity relationship for a series of nonviral gene delivery systems have been largely unsuccessful (Braun et al., 2003, 2005; Choosakoonkriang et al., 2003a; Lobo et al., 2001; Wiethoff et al., 2002, 2003, 2004). Transfection studies of both PDDCs and CLDCs indicate that complexes composed of moderate (G4–G7) generation PAMAM dendrimers or DOTAP liposomes provide the greatest biological activity (Braun et al., 2005; Kukowska-Latallo et al., 1996; Wiethoff et al., 2004). The activation energies of complex formation obtained here also show no obvious correlation with transfection efficiency. The kinetic behavior of dendrimer mediated complexation may best be considered in terms of two different classes of the polycations; the smaller G2 dendrimer and the larger G4–G9 molecules. For the series of higher generation dendrimers, the binding event follows the trend G4 > G7 > G9, whereas the opposite order was observed in the activation energies reflecting condensation events. Thus, we suggest a balance between a more energetically favorable condensation reaction and less favorable binding may prove beneficial to the competing needs of cellular uptake and dissociation of complexes within the cytoplasm.

REFERENCES

Akao, T., T. Fukumoto, H. Ihara, and A. Ito. 1996. Conformational change in DNA induced by cationic bilayer membranes. *FEBS Lett.* 391: 215–218.

Anchordoquy, T. J., L. G. Girouard, J. F. Carpenter, and D. J. Kroll. 1998. Stability of lipid/DNA complexes during agitation and freeze-thawing. *J. Pharm. Sci.* 87:1046–1051.

Bhattacharya, S., and S. S. Mandal. 1998. Evidence of interlipidic ion-pairing in anion-induced DNA release from cationic amphiphile-DNA complexes. Mechanistic implications in transfection. *Biochemistry.* 37: 7764–7777.

Bielinska, A. U., C. Chen, J. Johnson, and J. R. Baker, Jr. 1999. DNA complexing with polyamidoamine dendrimers: implications for transfection. *Bioconjug. Chem.* 10:843–850.

Bielinska, A. U., J. F. Kukowska-Latallo, and J. R. Baker, Jr. 1997. The interaction of plasmid DNA with polyamidoamine dendrimers: mechanism of complex formation and analysis of alterations induced in nuclease sensitivity and transcriptional activity of the complexed DNA. *Biochim. Biophys. Acta.* 1353:180–190.

Birchall, J. C., I. W. Kellaway, and S. N. Mills. 1999. Physico-chemical characterisation and transfection efficiency of lipid-based gene delivery complexes. *Int. J. Pharm.* 183:195–207.

Boussif, O., F. Lezoualc'h, M. A. Zanta, M. D. Mergny, D. Scherman, B. Demeneix, and J. P. Behr. 1995. A versatile vector for gene and oligonucleotide transfer into cells in culture and in vivo: polyethylenimine. *Proc. Natl. Acad. Sci. USA.* 92:7297–7301.

Braun, C. S., G. S. Jas, S. Choosakoonkriang, G. S. Koe, J. G. Smith, and C. R. Middaugh. 2003. The structure of DNA within cationic lipid/DNA complexes. *Biophys. J.* 84:1114–1123.

Braun, C. S., J. A. Vetro, D. A. Tomalia, G. Koe, J. G. Koe, and C. R. Middaugh. 2005. Structure/function relationships of polyamidoamine/DNA dendrimers as gene delivery vehicles. *J. Pharm. Sci.* 94:423–436.

Chen, W., N. J. Turro, and D. A. Tomalia. 2000. Using ethidium bromide to probe the interactions between DNA and dendrimers. *Langmuir.* 16:15–19.

Choosakoonkriang, S., B. A. Lobo, G. S. Koe, J. G. Koe, and C. R. Middaugh. 2003a. Biophysical characterization of PEI/DNA complexes. *J. Pharm. Sci.* 92:1710–1722.

Choosakoonkriang, S., C. M. Wiethoff, T. J. Anchordoquy, G. S. Koe, J. G. Smith, and C. R. Middaugh. 2001. Infrared spectroscopic characterization of the interaction of cationic lipids with plasmid DNA. *J. Biol. Chem.* 276:8037–8043.

Choosakoonkriang, S., C. M. Wiethoff, G. S. Koe, J. G. Koe, T. J. Anchordoquy, and C. R. Middaugh. 2003b. An infrared spectroscopic study of the effect of hydration on cationic lipid/DNA complexes. *J. Pharm. Sci.* 92:115–130.

Cosa, G., K. S. Focsaneanu, J. R. McLean, J. P. McNamee, and J. C. Scaiano. 2001. Photophysical properties of fluorescent DNA-dyes bound to single- and double-stranded DNA in aqueous buffered solution. *Photochem. Photobiol.* 73:585–599.

Crook, K., G. McLachlan, B. J. Stevenson, and D. J. Porteous. 1996. Plasmid DNA molecules complexed with cationic liposomes are protected from degradation by nucleases and shearing by aerosolisation. *Gene Ther.* 3:834–839.

Dunlap, D. D., A. Maggi, M. R. Soria, and L. Monaco. 1997. Nanoscopic structure of DNA condensed for gene delivery. *Nucleic Acids Res.* 25:3095–3101.

Eastman, S. J., C. Siegel, J. Tousignant, A. E. Smith, S. H. Cheng, and R. K. Scheule. 1997. Biophysical characterization of cationic lipid: DNA complexes. *Biochim. Biophys. Acta.* 1325:41–62.

Evans, H. M., A. Ahmad, K. Ewert, T. Pfohl, A. Martin-Herranz, R. F. Bruinsma, and C. R. Safinya. 2003. Structural polymorphism of DNA-dendrimer complexes. *Phys. Rev. Lett.* 91:075501.

Felgner, J. H., R. Kumar, C. N. Sridhar, C. J. Wheeler, Y. J. Tsai, R. Border, P. Ramsey, M. Martin, and P. L. Felgner. 1994. Enhanced gene delivery and mechanism studies with a novel series of cationic lipid formulations. *J. Biol. Chem.* 269:2550–2561.

Felgner, P. L., T. R. Gadek, M. Holm, R. Roman, H. W. Chan, M. Wenz, J. P. Northrop, G. M. Ringold, and M. Danielsen. 1987. Lipofection: a highly efficient, lipid-mediated DNA-transfection procedure. *Proc. Natl. Acad. Sci. USA.* 84:7413–7417.

Gershon, H., R. Ghirlando, S. B. Guttman, and A. Minsky. 1993. Mode of formation and structural features of DNA-cationic liposome complexes used for transfection. *Biochemistry.* 32:7143–7151.

Golan, R., L. I. Pietrasanta, W. Hsieh, and H. G. Hansma. 1999. DNA toroids: stages in condensation. *Biochemistry.* 38:14069–14076.

Harvie, P., F. M. Wong, and M. B. Bally. 1998. Characterization of lipid DNA interactions. I. Destabilization of bound lipids and DNA dissociation. *Biophys. J.* 75:1040–1051.

Huang, C. Y., S. S. Ma, S. Lee, R. Radhakrishnan, C. S. Braun, S. Choosakoonkriang, C. M. Wiethoff, B. A. Lobo, and C. R. Middaugh. 2002. Enhancements in gene expression by the choice of plasmid DNA formulations containing neutral polymeric excipients. *J. Pharm. Sci.* 91:1371–1381.

Huang, C. Y., T. Uno, J. E. Murphy, S. Lee, J. D. Hamer, J. A. Escobedo, F. E. Cohen, R. Radhakrishnan, V. Dwarki, and R. N. Zuckermann. 1998. Lipitoids: novel cationic lipids for cellular delivery of plasmid DNA in vitro. *Chem. Biol.* 5:345–354.

Koltover, I., T. Salditt, J. O. Radler, and C. R. Safinya. 1998. An inverted hexagonal phase of cationic liposome-DNA complexes related to DNA release and delivery. *Science.* 281:78–81.

Krishnamoorthy, G., G. Duportail, and Y. Mely. 2002. Structure and dynamics of condensed DNA probed by 1,1′-(4,4,8,8-tetramethyl-4,8-diazaundecamethylene)bis[4-[[3- methylbenz-1,3-oxazol-2-yl]methylidine]-1,4-dihydroquinolinium] tetraiodide fluorescence. *Biochemistry.* 41:15277–15287.

Kukowska-Latallo, J. F., A. U. Bielinska, J. Johnson, R. Spindler, D. A. Tomalia, and J. R. Baker, Jr. 1996. Efficient transfer of genetic material into mammalian cells using Starburst polyamidoamine dendrimers. *Proc. Natl. Acad. Sci. USA.* 93:4897–4902.

Lai, E., and J. H. van Zanten. 2001. Monitoring DNA/poly-l-lysine polyplex formation with time-resolved multiangle laser light scattering. *Biophys. J.* 80:864–873.

Lai, E., and J. H. van Zanten. 2002. Real time monitoring of lipoplex molar mass, size and density. *J. Controlled Release.* 82:149–158.

Larsson, A., C. Carlsson, M. Jonsson, and B. Albinsson. 1994. Characterization of the binding of the fluorescent dyes YO and YOYO to DNA by polarized light spectroscopy. *J. Am. Chem. Soc.* 116:8459–8465.

Lee, H., S. K. Williams, S. D. Allison, and T. J. Anchordoquy. 2001. Analysis of self-assembled cationic lipid-DNA gene carrier complexes using flow field-flow fractionation and light scattering. *Anal. Chem.* 73:837–843.

Lengsfeld, C. S., and T. J. Anchordoquy. 2002. Shear-induced degradation of plasmid DNA. *J. Pharm. Sci.* 91:1581–1589.

Levy, M. S., I. J. Collins, S. S. Yim, J. M. Ward, N. Titchener-Hooker, P. Ayazi Shamlou, and P. Dunnill. 1999. Effect of shear on plasmid DNA in solution. *Bioprocess Biosyst. Eng.* 20:7–13.

Levy, M. S., R. D. O'Kennedy, P. Ayazi-Shamlou, and P. Dunnill. 2000. Biochemical engineering approaches to the challenges of producing pure plasmid DNA. *Trends Biotechnol.* 18:296–305.

Lin, A. J., N. L. Slack, A. Ahmad, C. X. George, C. E. Samuel, and C. R. Safinya. 2003. Three-dimensional imaging of lipid gene-carriers: membrane charge density controls universal transfection behavior in lamellar cationic liposome-DNA complexes. *Biophys. J.* 84:3307–3316.

Lobo, B. A., A. Davis, G. Koe, J. G. Smith, and C. R. Middaugh. 2001. Isothermal titration calorimetric analysis of the interaction between cationic lipids and plasmid DNA. *Arch. Biochem. Biophys.* 386:95–105.

Lobo, B. A., G. S. Koe, J. G. Koe, and C. R. Middaugh. 2003. Thermodynamic analysis of binding and protonation in DOTAP/DOPE (1:1): DNA complexes using isothermal titration calorimetry. *Biophys. Chem.* 104:67–78.

Lobo, B. A., S. A. Rogers, S. Choosakoonkriang, J. G. Smith, G. Koe, and C. R. Middaugh. 2002. Differential scanning calorimetric studies of the thermal stability of plasmid DNA complexed with cationic lipids and polymers. *J. Pharm. Sci.* 91:454–466.

McKenzie, D. L., K. Y. Kwok, and K. G. Rice. 2000. A potent new class of reductively activated peptide gene delivery agents. *J. Biol. Chem.* 275:9970–9977.

Murphy, J. E., T. Uno, J. D. Hamer, F. E. Cohen, V. Dwarki, and R. N. Zuckermann. 1998. A combinatorial approach to the discovery of efficient cationic peptoid reagents for gene delivery. *Proc. Natl. Acad. Sci. USA.* 95:1517–1522.

Philip, R., D. Liggitt, M. Philip, P. Dazin, and R. Debs. 1993. In vivo gene delivery. Efficient transfection of T lymphocytes in adult mice. *J. Biol. Chem.* 268:16087–16090.

Radler, J. O., I. Koltover, T. Salditt, and C. R. Safinya. 1997. Structure of DNA-cationic liposome complexes: DNA intercalation in multilamellar membranes in distinct interhelical packing regimes. *Science.* 275:810–814.

Richter-Egger, D. L., A. Tesfai, and S. A. Tucker. 2001. Spectroscopic investigations of poly(propyleneimine)dendrimers using the solvatochromic probe phenol blue and comparisons to poly(amidoamine) dendrimers. *Anal. Chem.* 73:5743–5751.

Rye, H. S., S. Yue, D. E. Wemmer, M. A. Quesada, R. P. Haugland, R. A. Mathies, and A. N. Glazer. 1992. Stable fluorescent complexes of double-stranded DNA with bis-intercalating asymmetric cyanine dyes: properties and applications. *Nucleic Acids Res.* 20:2803–2812.

Tecle, M., M. Preuss, and A. D. Miller. 2003. Kinetic study of DNA condensation by cationic peptides used in nonviral gene therapy: analogy of DNA condensation to protein folding. *Biochemistry.* 42:10343–10347.

Wang, D., and T. Imae. 2004. Fluorescence emission from dendrimers and its pH dependence. *J. Am. Chem. Soc.* 126:13204–13205.

Wiethoff, C. M., M. L. Gill, G. S. Koe, J. G. Koe, and C. R. Middaugh. 2002. The structural organization of cationic lipid-DNA complexes. *J. Biol. Chem.* 277:44980–44987.

Wiethoff, C. M., M. L. Gill, G. S. Koe, J. G. Koe, and C. R. Middaugh. 2003. A fluorescence study of the structure and accessibility of plasmid DNA condensed with cationic gene delivery vehicles. *J. Pharm. Sci.* 92:1272–1285.

Wiethoff, C. M., J. G. Koe, G. S. Koe, and C. R. Middaugh. 2004. Compositional effects of cationic lipid/DNA delivery systems on transgene expression in cell culture. *J. Pharm. Sci.* 93:108–123.

Wiethoff, C. M., J. G. Smith, G. S. Koe, and C. R. Middaugh. 2001. The potential role of proteoglycans in cationic lipid-mediated gene delivery. Studies of the interaction of cationic lipid-DNA complexes with model glycosaminoglycans. *J. Biol. Chem.* 276:32806–32813.

Wong, F. M., P. Harvie, Y. P. Zhang, E. C. Ramsay, and M. B. Bally. 2003. Phosphatidylethanolamine mediated destabilization of lipid-based pDNA delivery systems. *Int. J. Pharm.* 255:117–127.

Wong, M., S. Kong, W. H. Dragowska, and M. B. Bally. 2001. Oxazole yellow homodimer YOYO-1-labeled DNA: a fluorescent complex that can be used to assess structural changes in DNA following formation and cellular delivery of cationic lipid DNA complexes. *Biochim. Biophys. Acta.* 1527:61–72.

Zaric, V., D. Weltin, P. Erbacher, J. S. Remy, J. P. Behr, and D. Stephan. 2004. Effective polyethylenimine-mediated gene transfer into human endothelial cells. *J. Gene Med.* 6:176–184.

Zhu, N., D. Liggitt, Y. Liu, and R. Debs. 1993. Systemic gene expression after intravenous DNA delivery into adult mice. *Science.* 261: 209–211.

Zuidam, N. J., Y. Barenholz, and A. Minsky. 1999. Chiral DNA packaging in DNA-cationic liposome assemblies. *FEBS Lett.* 457: 419–422.